https://doi.org/10.5194/gmd-2020-274
Preprint. Discussion started: 4 September 2020


Geoscientific Model Development Discussions

# Influence of biomass burning vapor wall loss correction on modeling organic aerosols in Europe by CAMx v6.50

Jianhui Jiang[1], Imad El Haddad[1], Sebnem Aksoyoglu[1], Giulia Stefenelli[1], Amelie Bertrand[1,2], Nicolas Marchand[2], Francesco Canonaco[1], Jean-Eudes Petit[3], Olivier Favez[3], Stefania Gilardoni[4], Urs Baltensperger[1], André S. H. Prévôt[1]

[1]Laboratory of Atmospheric Chemistry, Paul Scherrer Institute, 5232 Villigen PSI, Switzerland
[2]Aix Marseille Univ, CNRS, LCE, Marseille, France
[3]Institut National de l'Environnement Industriel et des Risques (INERIS), Verneuil-en-Halatte, France
[4]Italian National Research Council – Institute of Polar Sciences, Bologna, Italy

*Correspondence to*: Imad El Haddad (imad.el-haddad@psi.ch), Sebnem Aksoyoglu (sebnem.aksoyoglu@psi.ch) and Jianhui Jiang (jianhui.jiang@psi.ch)

**Abstract.** Increasing evidence from experimental studies suggests that the losses of semi-volatile vapors to the chamber walls could be responsible for the underestimation of organic aerosol (OA) in air quality models which use parameters obtained from the chamber experiments. In this study, a box model with volatility basis set (VBS) scheme was developed and the secondary organic aerosol (SOA) yields with vapor wall loss corrected were optimized by a genetic algorithm based on advanced chamber experimental data for biomass burning. The vapor wall loss correction increases the SOA yields by a factor of 1.9–4.9, and leads to a better agreement with the measured OA for 14 chamber experiments under different temperatures and emission loads. To investigate the influence of vapor wall loss correction on regional OA simulations, the optimized parameterizations (SOA yields, emissions of intermediate-volatility organic compounds from biomass burning, and enthalpy of vaporization) were implemented in the regional air quality model CAMx (Comprehensive Air Quality Model with extensions). The modeled results from the standard and vapor wall loss corrected VBS schemes, as well as the traditional two-product approach were compared and evaluated by OA measurements from five Aerodyne aerosol chemical speciation monitor (ACSM)/aerosol mass spectrometer (AMS) stations in the winter of 2011. The vapor wall loss corrected VBS (VBS_WLS) generally shows the best performance for predicting OA among all OA schemes, and reduces the mean fractional bias from -72.9% (with the standard VBS (VBS_BASE)) to -1.6% for the winter OA. In Europe, the VBS_WLS produces the highest domain average OA in winter (2.3 μg $m^{-3}$), which is 106.6% and 26.2% higher than the standard VBS and the reference scenario (VBS_noWLS, same parameterization as VBS_WLS, except with the default yields without vapor wall loss correction), respectively. Compared to VBS_noWLS, VBS_WLS leads to an increase in SOA by up to ~80% in Romania. VBS_WLS also leads to a better agreement between the modeled SOA fraction in OA (fSOA) and the estimated measured values in the literature. The substantial influence of vapor wall loss correction on modeled OA in Europe highlights the importance of further improvements in the parameterizations based on laboratory studies with a wider range of chamber conditions and field observations with higher spatial and temporal coverage.

https://doi.org/10.5194/gmd-2020-274
Preprint. Discussion started: 4 September 2020


Geoscientific Model Development Discussions

## 1 Introduction

Organic aerosol (OA) accounts for a substantial fraction of atmospheric particulate matter (Jimenez et al., 2009), which is closely associated with human health impacts and climate change (Cohen et al., 2017; Kanakidou et al., 2005; Lelieveld et al., 2015). Organic aerosol originates from a variety of natural and anthropogenic sources (Hallquist et al., 2009), among which residential biomass burning emission has been recognized as the dominant source for both primary (POA) and secondary (SOA) organic aerosols in winter (Butt et al., 2016; Jiang et al., 2019b; Qi et al., 2019). Despite its substantial contribution to OA, biomass burning OA is largely underestimated by chemical transport models (CTM) (Hallquist et al., 2009; Robinson et al., 2007).

Many efforts have been devoted to understand and diminish the gap between modeled and observed OA from biomass burning. One of the major reasons of the underestimated OA is the absence of semi-volatile organic compounds (SVOCs) from residential biomass burning in the current emission inventories (Denier van der Gon et al., 2015). A smog-chamber study showed that the precursors traditionally included in the CTMs account for only ~3-27% of the observed SOA from residential biomass burning (Bruns et al., 2016). In order to compensate the effects from missing precursors, various modeling studies increased the POA emissions by a factor based on findings from chamber experiments (Ciarelli et al., 2017a; Fountoukis et al., 2014; Jiang et al., 2019b; Tsimpidi et al., 2010). Meanwhile, increasing evidence from chamber experiments demonstrated that the losses of semi-volatile vapors to the chamber walls could lead to a substantial underestimation of OA (Bertrand et al., 2018; Bian et al., 2015; Krechmer et al., 2016; Loza et al., 2010; Matsunaga and Ziemann, 2010; Zhang et al., 2014). Unlike the particle wall losses – which have been routinely corrected in the chamber studies – the effects of vapor wall losses are rarely investigated and considered in modeling practices.

Zhang et al. (2014) reported that the vapor wall losses may lead to an underestimation of SOA by a factor of 4 based on laboratory chamber data. This factor has been adopted by several CTM studies to scale the yields of SOA up. For instance, Baker et al. (2015) tested the sensitivity of CMAQ to the vapor wall loss by increasing the yields of semi-volatile gases by a factor of 4, in which the traditional two-product approach was used for OA simulations. This factor was also implemented in a CTM with volatility basis set (VBS) scheme (Hayes et al., 2015), which distributed organic species into logarithmically spaced volatility bins and was shown to improve the model performance for predicting SOA (Donahue et al., 2006; Donahue et al., 2011; Hodzic et al., 2010; Robinson et al., 2007). Nevertheless, additional laboratory studies showed that the wall loss factor could be even higher than 4 according to different chamber conditions (Akherati et al., 2019; Krechmer et al., 2016). On the other hand, some studies took the vapor wall loss corrections into account in CTMs using the SOA yields generated from the Statistical Oxidation Model (SOM). Cappa et al. (2016) and Akherati et al. (2019) used the traditional two-product model to fit vapor wall loss corrected SOA yields, and applied the yields in the regional CTM UCD/CIT. They reported, however, that the two-product fits might not be sufficiently robust. Furthermore, Hodzic et al. (2016) used a vapor wall loss corrected VBS parameterization in the global model GEOS-Chem based on chamber experiments conducted on individual

https://doi.org/10.5194/gmd-2020-274
Preprint. Discussion started: 4 September 2020


Geoscientific Model Development Discussions

precursors, which are highly dependent on the experimental conditions. Each of these latter studies clearly called for a better assessment of the uncertainties across the entire range of precursor compounds as well as under different chamber conditions.

Here, we 1) developed a VBS-based box model and fit the vapor wall loss corrected SOA yields of biomass burning IVOC based on the 14 chamber experiments under different temperature and emission loads, 2) implemented the vapor wall loss corrected VBS parameters in the regional chemical transport model Comprehensive Air Quality Model with extensions (CAMx), and 3) investigated the role of vapor wall loss correction on model performance by comparing modeled organic aerosols from traditional and modified VBS OA schemes with ambient observations at multiple European sites.

## 2. Parameterization method

### 2.1 Chamber experimental data

The parameterization of the VBS scheme was based on experimental data from two smog chamber campaigns in 2014-2015. It includes 14 datasets from experiments conducted under various temperature conditions (-10°C, 2°C, 15°C) and covered a wide range of emission loads (from 19 to 284 μg $m^{-3}$). Emissions were generated by combustion of beech wood in three different wood stoves including conventional and modern burners manufactured in 2002-2010. The organic gases covering 86 intermediate-volatility and semi-volatile organic compounds (S/IVOC) which are SOA precursors, were measured by a proton-transfer-reaction time-of-flight mass spectrometer (PTR-ToF-MS). The aerosol evolution was monitored by a high-resolution time-of-flight aerosol mass spectrometer (HR-ToF-AMS). A detailed description of the experiments can be found in Stefenelli et al. (2019), Bertrand et al. (2017) and Bruns et al. (2016).

### 2.2 VBS box model

A VBS box model was developed to simulate the formation and evolution of primary and secondary OA in the chamber. We assumed that the condensable gases generated from oxidation of the precursors could 1) partition to the particle phase, 2) be lost on the chamber wall, as well as 3) be diluted. The organic compounds were distributed into 6 logarithmically spaced volatility bins, corresponding to saturation concentrations of $10^{-1}$, $10^{0}$, $10^{1}$, $10^{2}$, $10^{3}$, and $10^{4}$ μg $m^{-3}$. The change in the organic gas concentration ($C$) for a constituent within the volatility bin $i$ ($C_i$) can be described by Eq. (1), where $P$ is the production of organic gas (OG) in the chamber due to oxidization of precursors, $k_{cs}$ is the condensation sink ($s^{-1}$) describing the speed of condensable gases condensing on existing aerosol particles, $k_w$ is the rate constant of vapor lost to the wall, $k_{dil}$ is the dilution rate, and $Ceq_{i,p}$ and $Ceq_{i,w}$ represent the gas-phase equilibrium concentrations at the aerosol particles and chamber wall surface, respectively:

$$\frac{dC_i}{dt} = P \cdot \zeta_i - k_{cs}\left(C_i - Ceq_{i,p}\right) - k_w\left(C_i - Ceq_{i,w}\right) - k_{dil} \cdot C_i \quad (1)$$

https://doi.org/10.5194/gmd-2020-274
Preprint. Discussion started: 4 September 2020


Geoscientific Model Development Discussions

The production rates of oxidized organic gases $P$ is determined by the measured consumption rates of precursors taking into account their dilution. $\zeta_i$ represents the mass fraction of primary and oxidation products in a volatility bin $i$. $\zeta_i$ of POA from biomass burning is obtained from May et al. (2013), with values of 0.2, 0.1, 0.1, 0.2, 0.1, 0.3 for compounds in each volatility bin. $\zeta_i$ of oxidation products are assumed to follow a kernel normal distribution as a function of $logC^*$, $\zeta \sim N(\mu, \sigma^2)$, where $\mu$ is the median value of log$C^*$ and $\sigma$ is the standard deviation, which will be optimized as described in Section 2.3. The time series of $k_{dil}$ is obtained from Stefenelli et al. (2019). The $k_{cs}$ of each experiment is obtained from Bertrand et al. (2018). We tested three $k_w$ values 0.0020 $s^{-1}$, 0.0033 $s^{-1}$, 0.0040 $s^{-1}$, covering the entire range determined by Bertrand et al. (2018) for our chamber, as well as a base case assuming there is no vapor wall loss in the chamber ($k_w$ = 0). The condensation of a species in the particle-phase ($C_p$) can then be described by Eq. (2).

$$\frac{dC_{i,p}}{dt} = k_{cs}\left(C_i - Ceq_{i,p}\right) - k_{dil} \cdot C_{i,p} \quad (2)$$

Following the partitioning model of Pankow (1994), the gas-phase equilibrium concentrations in particle phase ($Ceq_{i,p}$) and at the chamber wall ($Ceq_{i,w}$) are determined by their partitioning coefficients $\xi_i$ and $\xi_{i,w}$ (Donahue et al., 2009), as shown in Eq. (3) and Eq. (4):

$$Ceq_{i,p} = (C_{i,g} + C_{i,p}) \cdot [1 - \xi_i], \quad \xi_i = \left(1 + \frac{C_i^*}{C_{OA}}\right)^{-1} \quad (3)$$

$$Ceq_{i,w} = (C_{i,g} + C_{i,w}) \cdot [1 - \xi_{i,w}], \ \xi_{i,w} = \left(1 + \frac{C_i^*}{C_{wall}}\right)^{-1} \quad (4)$$

where $C^*$ represents the saturation concentration, $C_{OA}$ is the wall-loss corrected OA concentration measured by the AMS, $C_{wall}$ is the equivalent organic mass concentration at the wall determined in Bertrand et al. (2018). The Clausius-Clapeyron equation (Eq. 5) was applied to take into account the effects of temperature on $C^*$:

$$C^* = C_{T0}^* \cdot \frac{T_0}{T} \cdot exp\left(\frac{\Delta H_{vap}/8.314}{1/T_0 - 1/T}\right) \quad (5)$$

where $C_{T0}^*$ is the mass saturation concentration under the reference temperature ($T_0$). $T$ is the temperature of each experiment, while $T_0$ equals 298 K. $\Delta H_{vap}$ (J) is the enthalpy of vaporization at reference temperature, and 8.314 is the universal gas constant (J $mol^{-1}$ $K^{-1}$). $\Delta H_{vap} = \{70000 - 11000 \times \log C^*\}$ is adopted for the primary set (May et al., 2013), while $\Delta H_{vap}$ of the oxidized products is determined during model optimization. The $C_{wall}$ was determined in previous studies as on the order of a few mg $m^{-3}$ (Bertrand et al., 2018). In this study, we run the box model for three different $C_{wall}$ values (1, 5, 25 mg $m^{-3}$) with a reference temperature of 2 °C (275.15 K) according to Bertrand et al. (2018).

### 2.3 Model optimization

The model is optimized to constrain the volatility distribution (as a function of $logC^*$, $\zeta \sim N(\mu, \sigma^2)$) and $\Delta H_{vap}$ of the oxidized products. A genetic algorithm (GA) is used to find the best-fit parameters leading to the lowest average root-mean-square error (RMSE) and mean bias (MB) between modeled and measured OA concentrations for all 14 experiments. The genetic algorithm is a metaheuristic algorithm inspired by the natural selection process to generate optimized solutions (Mitchell, 1996). It begins

https://doi.org/10.5194/gmd-2020-274
Preprint. Discussion started: 4 September 2020


Geoscientific Model Development Discussions

by creating an initial population of individual solutions (20 different combinations of $\mu$, $\sigma$, $\Delta H_{vap}$ here) within certain upper and lower bounds, as called parents. The performance of each solution is evaluated by a fitness function, which is the sum of RMSE and MB between modeled and measured OA concentrations of 14 experiments in this study. A new generation of solutions is then formed either by making random changes to a single parent (called mutation) or by combining the vector entries of a pair of parents (called crossover). The process will be repeated until reaching the stopping conditions, which are either the iterations time reaching 50 or the stall generations (generation with no significant change of fitness function) reaching 20. The GA is conducted using the genetic algorithm solver of Global Optimization Toolbox of MATLAB R2019a (The MathWorks, Inc).

## 3. Modeling approach

### 3.1 Regional chemical transport model CAMx

The regional model CAMx version 6.50 (Ramboll, 2018) was used to model organic aerosol in Europe (15°W – 35°E, 35°N – 70°N) for the whole year of 2011, with a horizontal resolution of 0.25° × 0.125° and 14 terrain following vertical layers from ~20 m above ground reaching up to 460 hPa. The Carbon Bond 6 Revision 2 (CB6r2) gas-phase mechanism (Hildebrandt Ruiz and Yarwood, 2013) was selected. The gas-aerosol partitioning of inorganic aerosols was simulated by the ISORROPIA thermodynamic model (Nenes et al., 1998). For organic aerosols, several OA schemes including both the traditional 2-product approach (SOA chemistry/partitioning scheme, SOAP) and the VBS scheme with different parameterizations were applied (see Section 3.2).

The meteorological parameters were prepared with the Weather Research and Forecasting model (WRF, version 3.7.1; Skamarock et al., 2008) based on the 6-h European Centre for Medium–Range Weather Forecasts (ECMWF) reanalysis global data (Dee et al., 2011). The meteorological parameters were evaluated and reported in a previous study (Jiang et al., 2019a), which showed that most of the meteorological parameters met the criteria for meteorological model performance by Emery (2001). The initial and boundary conditions were obtained from the global model MOZART-4/GEOS-5 (Horowitz et al., 2003). Inputs of ozone column densities were produced based on the Total Ozone Mapping Spectrometer (TOMS) data by the National Aeronautics and Space Administration (NASA, ftp://toms.gsfc.nasa.gov/pub/omi/data/), and the photolysis rates were then calculated by the Tropospheric Ultraviolet and Visible (TUV) Radiation Model version 4.8 (NCAR, 2011). The source specific anthropogenic emissions were based on the European emission inventory TNO-MACC (Monitoring Atmospheric Composition and Climate)-III (Kuenen et al., 2014). The biogenic emissions (isoprene, monoterpenes, sesquiterpenes, soil NO) were simulated by the PSI model developed at the Laboratory of Atmospheric Chemistry at the Paul Scherrer Institute (Andreani-Aksoyoglu and Keller, 1995; Jiang et al., 2019a; Oderbolz et al., 2013). More details about the model inputs can be found in our previous studies performed using the same input data (Jiang et al., 2019a; Jiang et al., 2019b).

https://doi.org/10.5194/gmd-2020-274
Preprint. Discussion started: 4 September 2020


Geoscientific Model Development Discussions

### 3.2 Parameterization of OA schemes

To investigate the effects of vapor wall loss corrected yields, we modeled the OA in Europe by VBS schemes with three modified parameterizations, as well as the standard VBS parameterization (VBS_BASE) and a two-product approach (SOAP2.1) as base cases to compare with.

- *SOAP*. The SOAP (SOA chemistry/partitioning) module is a semi-volatile equilibrium scheme based on the traditional two-product approach. The POA emissions are assumed to be inert in SOAP. The updated parameterization of SOAP2.1 in CAMx v6.50 used the aerosol yield data that correct for vapor wall losses in smog chamber experiments based on Zhang et al. (2014).
- *VBS_BASE*. The VBS_BASE used the standard VBS parameterization in CAMx v6.50. The IVOC emissions from different sources were calculated based on literature. The IVOCs from gasoline and diesel vehicles were calculated as 25% and 20% of NMVOC emissions from gasoline and diesel vehicles, respectively (Jathar et al., 2014). IVOC emissions from residential biomass burning were estimated as 4.5 times of POA emissions based on Ciarelli et al. (2017a). The IVOC emissions from other anthropogenic sources were calculated as 1.5 times of POA as proposed by Robinson et al. (2007).
- *VBS_3POA*. An increasing number of studies have reported a considerable contribution of semi-volatile organic compounds (SVOCs) to SOA formation (Ciarelli et al., 2017b; Denier van der Gon et al., 2015; Woody et al., 2015). SVOCs are absent in the current emission inventories. Following the routine approach to offset the influence of missing SVOC emissions in previous studies, we increased the POA emissions by 3 times in VBS_3POA while keeping the other parameters the same as the standard VBS parameterization in CAMx v6.50. The VBS_BASE IVOC emissions were adopted here.
- *VBS_WLS*. The VBS_WLS used the optimized parameters by the VBS box model, including the emissions and vapor wall loss corrected yields for IVOC from residential biomass burning, and the $\Delta H_{vap}$ of the oxidized products. Based on the chamber measurements, the IVOC emissions from residential biomass burning is ~14 times the primary OM load (Fig. S1). To avoid the double counting of toluene, xylene and benzene emissions, which are already included in the emission inventory, we applied a factor of 12 to calculate the IVOC emissions from biomass burning. The IVOC emissions from other sources were estimated by the same approach as in VBS_3POA.
- *VBS_noWLS*. The VBS_noWLS was designed as a reference of VBS_WLS, which adopted the same parameters as VBS_WLS except for the yields. The VBS_noWLS used the fitted yields from the box model assuming that there is no vapor wall loss ($k_w = 0$).

### 3.3 Model evaluation

The general model performance for the major air pollutants ($SO_2$, $NO_2$, $O_3$, $PM_{2.5}$) was reported in our previous study (Jiang et al., 2019b), which was comparable to other modeling studies in Europe. OA measurements and source apportionment studies

https://doi.org/10.5194/gmd-2020-274
Preprint. Discussion started: 4 September 2020


Geoscientific Model Development Discussions

using positive matrix factorization (PMF) analysis from five Aerodyne aerosol chemical speciation monitor (ACSM) /aerosol mass spectrometer (AMS) stations in winter of 2011 were used to evaluate the modeled primary and secondary organic aerosol by different OA schemes: Zurich (Canonaco et al., 2013), Marseille (Bozzetti et al., 2017), SIRTA (Site Instrumental de Recherche par Télédétection Atmosphérique) facility located in the Paris region (Zhang et al., 2019), as well as Bologna and San Pietro Capofiume (SPC) (Paglione et al., 2020). For Zurich and SIRTA, only data collected from late autumn to early spring (January, February, March, November and December) - when emissions from biomass burning are relatively high - were used for the statistical analysis, although the observations covered longer time periods. The spatial distribution and observation periods of each station are shown in Fig. S2. The statistical metrics including mean bias (MB), mean error (ME), root-mean-square error (RMSE), mean fractional bias (MFB) and mean fractional error (MFE) between modeled and observed primary and secondary OA were calculated.

## 4. Results and discussion

### 4.1 Modeled and measured OA from chamber experiments

The optimized parameters were then applied to the box model to simulate OA production for 14 chamber experiments. Figure 1 shows the comparison between measured OA and modeled primary and secondary OA under the median chamber conditions ($k_w$ = 0.0033 $s^{-1}$, $C_{wall}$ = 5 mg $m^{-3}$) for each experiment. The model reproduces the process of OA formation for most of the experiments well, except for experiment #9 and #14 which have relatively lower OM loads (26 and 48 μg $m^{-3}$ for Exp9 and Exp14, respectively). While the model simulation without vapor wall loss correction largely overestimates the OA at the initial time point and underestimates the final OA (Fig. S3), the results were improved when the vapor wall loss is taken into account. The mean bias (MB) and root mean square error (RMSE) between the modeled and observed OA in 14 experiments are 6.7 μg $m^{-3}$ and 42.2 μg $m^{-3}$ for the case under median chamber conditions, which are 48% and 12% lower than in the case without vapor loss correction (MB = -12.8 μg $m^{-3}$, 47.8 μg $m^{-3}$). To investigate the role of vapor wall loss on the modeled OA, another set of simulations were performed, in which we used the same optimized parameterization under the median chamber conditions but set $k_w$ = 0. In these cases, the modeled OA concentrations (dashed line in Fig. 1) were based on the assumption that there is no vapor wall loss. The wall loss ratio $R_{wall}$, which is defined as the ratio between modeled OA concentration without ($k_w$ = 0) and with ($k_w$ = 0.0033 $s^{-1}$, $C_{wall}$ = 5 mg $m^{-3}$) vapor wall loss, was calculated for the endpoint of each experiment (Fig. 1c). The $R_{wall}$ values varied from 1.5 (Exp2) to 3.2 (Exp11) among the 14 experiments, and showed a clear dependence on the initial OA loads.

To further understand the factors influencing $R_{wall}$, we conducted a series of model simulations with and without vapor wall loss under different initial organic mass load, temperature and condensation sink inputs (Fig. 2). Higher $k_w$ and $C_{wall}$ lead to higher $R_{wall}$ values for all the cases, and different chamber conditions ($k_w$, $C_w$) could result in a different $R_{wall}$ by a factor of 1.2–1.6, depending on different temperature, OM loads and condensation sinks. The $R_{wall}$ values generally decrease with increasing initial OM loads, which is consistent with the fact that $R_{wall}$ values for Exp8–14 are higher than Exp1–7. The

https://doi.org/10.5194/gmd-2020-274
Preprint. Discussion started: 4 September 2020


Geoscientific Model Development Discussions

increased $R_{wall}$ with the increasing temperature explains why the Exp10–14 (T = 15 °C) have higher $R_{wall}$ than Exp8 and Exp9 (T = –10 °C) while they have similar OM load levels. The condensation sink is inversely correlated with $R_{wall}$, indicating that the higher the rate of condensable gases condensing on the existing particles, the lower the vapor loss to the chamber wall, and therefore the lower the effect of vapor wall loss on modeled OA.

The optimized volatility distribution for the secondary condensable gases from biomass burning (ppm per ppm IVOC) with and without vapor wall loss corrections are displayed in Fig. 3a. The vapor wall loss correction leads to a 3.3 times higher mass in the low-volatility bins ($logC^* \leq 0$), indicating significant effects of vapor wall loss correction on predicting the SOA production. To give a more direct view about the effects of vapor wall loss on the SOA yield, we integrated the mass of SOA for all the volatility bins at 298 K (Fig. 3b). The mass yield under the median chamber conditions for vapor wall loss ($k_w$ = 0.0033 $s^{-1}$, $C_{wall}$ = 5 mg $m^{-3}$) is higher than the base case without considering the vapor wall loss about by factors of 4.9 (when $C_{OA}$ = 0.1 μg $m^{-3}$) to 1.9 (when $C_{OA}$ = 1000 μg $m^{-3}$). The influence of vapor wall loss on mass yield decreases with decreasing temperature. At 0 °C, the mass yield with vapor wall loss correction is higher than the base case by factors of 4.3 (when $C_{OA}$ = 0.1 μg $m^{-3}$) to 1.7 (when $C_{OA}$ = 1000 μg $m^{-3}$).

### 4.2 Performance of CAMx with different OA schemes

The modeled OA concentrations with different OA schemes were compared with measurements from five ACSM/AMS stations in winter. The statistical results are shown in Table 1, and the distributions of OA concentrations and mean bias between modeled and measured primary and secondary OA are displayed in Fig. 4. The OA are overall underestimated with all OA schemes. The VBS schemes lead to a better model performance than the two-product approach SOAP, except for VBS_BASE with default VBS parameterization. These results are consistent with a previous study using CAMx (Meroni et al., 2017), in which the better performance of SOAP compared to the default VBS was reported as a result of error compensation. The improved performance of modified VBS (3POA, noWLS, WLS) for OA mainly comes from the contribution of SOA (Table 1). The modeled SOA by 3POA and noWLS are very similar, therefore the analysis below will focus on the comparison between noWLS and WLS, for which the only difference is that WLS uses vapor wall loss corrected yields for IVOCs from biomass burning while noWLS uses the fitted yields assuming no vapor wall loss ($k_w$=0). WLS reduces the MFB between the modeled and measured SOA from 52.5% in noWLS to 20.0%. WLS shows a better average MB than noWLS, however, also increases the upper whisker of the MB (Fig. 4b), largely affected by overestimated SOA in Bologna and SPC.

Limited by the availability of OA measurements, the effects of vapor wall loss correction on model performance present a clear site dependence in this study. The modeled and measured daily average OA concentrations at each site are shown in Fig. 5. The temporal variations of primary and secondary OA at these sites can be found in Fig. S4. VBS_WLS leads to the best performance for both OA and SOA in Marseille and SIRTA, in spite of an overall underestimation (Fig. S4b, c). In Zurich, the vapor wall loss corrected yields for biomass burning improve the model performance in February and March, while there is an overestimation of the OA and SOA for all the OA schemes in November (Fig. S4a). The largest contribution to OA during

https://doi.org/10.5194/gmd-2020-274
Preprint. Discussion started: 4 September 2020


Geoscientific Model Development Discussions

this period was found to be from the biogenic SOA, which was potentially overestimated due to the overestimated temperatures during the same time period (Jiang et al., 2019b). Bologna and SPC are located in the Po Valley where biomass burning contributes most to the winter OA (Jiang et al., 2019b), and therefore higher effects from vapor wall loss correction on SOA are observed compared to other sites. At SPC, the fog scavenging processes played an important role on OA during the measurements (Gilardoni et al., 2014), however, the meteorological model failed to reproduce the fog events due to the coarse resolution in this study (Jiang et al., 2019b). Consequently, both VBS_WLS and noWLS lead to an overestimation of OA and SOA, while SOAP and VBS_BASE show better performance probably due to compensation of errors (Fig. S4e). In Bologna, a significant overestimation of temperature was found on 2 to 6 December (Jiang et al., 2019b), leading to a significant underestimation of SOA for all the OA schemes (Fig. S4d). Excluding this period, the modeled SOA by VBS_WLS is 89% higher than the measurements, while the modeled SOA concentrations by the other schemes are closer to the measurements with relative differences of -64% for SOAP, -10% for VBS_BASE, and 4% for VBS_noWLS.

The distinct performance of vapor wall loss corrected VBS at different sites could arise from various reasons. It might come from the high uncertainties of S/IVOC emissions from biomass burning, which were estimated by the same factor for the whole domain but were reported to have substantial inter-country variations (Denier van der Gon et al., 2015). Missing formation and removal processes such as photolytic and heterogeneous oxidation in the model could also result in different model performance for specific sites. In addition, in spite of the advanced chamber measurements we used to optimize the yield parameters, covering a wide range of precursor species and multiple temperature and chamber conditions, the fitted vapor wall loss corrected parameterization is still highly uncertain. To achieve a more robust parameterization and to further improve the model performance for OA, more studies on S/IVOC emissions, as well as the formation and removal mechanisms of SOA based on extensive laboratory studies and field observations with higher spatial and temporal coverage are needed.

### 4.3 Effects of vapor wall loss correction on modeled OA in Europe

#### 4.3.1 OA

The modeled OA results in Europe for the whole year 2011 by different OA schemes were compared to investigate the effects of OA schemes and the vapor wall loss correction. Figure 6 shows the modeled OA, SOA and POA in winter (December–January–February). VBS_WLS leads to the highest domain average OA (2.3 μg $m^{-3}$), which is 16.4%, 26.2%, 38.7% and 106.6% higher than VBS_3POA, VBS_noWLS, SOAP and VBS_BASE, respectively. The VBS schemes generally produce higher OA than SOAP, except for the default parameterization (VBS_BASE) in which the lack of SVOC emissions is not considered. However, SOAP leads to the second highest SOA after VBS_WLS, especially in northern Europe where the monoterpene emissions from coniferous forests are relatively high. This is mostly because of the high terpene SOA yields in SOAP2.1, which were reduced in the later version of the CAMx model (CAMx v7.0, http://www.camx.com). The vapor wall loss corrected yields lead to increased SOA in large areas of central and southern Europe (Fig. 7). The largest difference is predicted for the Po Valley and Romania regions with high residential biomass burning impact. The overall relative differences

https://doi.org/10.5194/gmd-2020-274
Preprint. Discussion started: 4 September 2020


Geoscientific Model Development Discussions

are more than 80% and the highest grid-scale increment reaches 5.6 μg $m^{-3}$ in Romania. The modeled POA concentrations are similar to those in the VBS case with correction for SVOC (3POA, noWLS, WLS) with domain average concentrations ranging from 0.9 (noWLS) to 1.1 (3POA) μg $m^{-3}$, and therefore no significant effects were observed from vapor wall loss correction (Fig. 7). The POA simulated by VBS_BASE (0.3 μg $m^{-3}$) is even lower than SOAP (0.7 μg $m^{-3}$), as the POA is semi-volatile and could evaporate and react with oxidants to form secondary products in VBS while SOAP assumes the POA to be inert.

The effects of different VBS schemes on OA are much smaller in summer (Fig. S5). Despite a slight increase from the VBS_BASE (1.2 μg $m^{-3}$), the modeled OA by the three modified VBS schemes are quite similar (1.4 – 1.5 μg $m^{-3}$). The effects of vapor wall loss corrected yields for biomass burning emissions are negligible due to low emissions in summer (Fig. S6). SOAP produced the highest OA (2.1 μg $m^{-3}$) in summer due to the high SOA yields from monoterpenes as explained before.

#### 4.3.2 Fraction of SOA in OA

The effects of the updated VBS schemes on the fraction of annual average SOA in total OA (fSOA = SOA/OA) are shown in Fig. 8. The VBS schemes lead to a higher fSOA (domain average 71.4%–87.3%) compared to SOAP (domain average 69.9%) in most of the domain except for northern Europe, where SOAP produces high biogenic SOA. The increased POA emissions to offset the missing SVOC emissions (3POA, noWLS, WLS) decrease the fSOA compared to the default VBS parameterization (BASE), while the vapor wall loss correction yields (WLS) result in ~5.8% higher fSOA than noWLS for the domain average and the largest grid-scale increase reaches 43.4% in the Balkans. The absolute differences between fSOA for WLS and noWLS are relatively higher in rural areas than urban areas, where fSOA is lower due to high primary emissions.

The modeled fSOA values were compared with the measurements from previous studies in Europe (Crippa et al., 2014; Jiang et al., 2019b). The measured fSOA from literature covered 18 sites and different seasons between 2008 and 2011 (Table S1). SOAP tends to underestimate the fSOA, while VBS_BASE significantly over-predicts the fSOA (Fig. 9). Both WLS and noWLS tend to underestimate the high fSOA and overestimate the low fSOA. VBS_WLS has 5% higher fSOA than VBS_noWLS and shows the highest agreement on the range of fSOA with the measurements, as well as the average fSOA values (measured: 69.6%; VBS_WLS: 69.1%). The largest improvements occur in winter, when the vapor wall corrected yields of biomass burning emissions largely increase the SOA production.

## 5. Conclusions

In this study, we optimized the SOA yields for a VBS-based box model using 14 chamber experiments with biomass burning and implemented the fitted VBS parameters (SOA yields, IVOC emissions from biomass burning, and enthalpy of vaporization) in the regional air quality model CAMx v6.5. The influence of the vapor wall loss correction on the model performance was investigated by comparing modeled primary and secondary OA with the traditional and modified OA schemes, including the 2-product approach (SOAP), the standard VBS (VBS_BASE), VBS with 3 times of POA to compensate for the missing SVOC (VBS_3POA), VBS with vapor wall loss correction (VBS_WLS) and an additional reference scenario

https://doi.org/10.5194/gmd-2020-274
Preprint. Discussion started: 4 September 2020


Geoscientific Model Development Discussions

with the same parameterizations as in VBS_WLS except for using the default SOA yields from biomass burning IVOC (VBS_noWLS).

The vapor wall loss correction increases the mass distributed in the low-volatility bins ($logC^* \leq 0$) by a factor of 4.3, and increases the SOA yields by a factor of 1.9–4.9 (at 298 K). Comparison of the modeled results with different OA schemes with the field measurements from five ACSM/AMS stations in Europe in winter, suggests that VBS_WLS generally has the best performance to predict OA, which lowers the mean fractional bias from -72.9% (VBS_BASE) to -1.6% for OA, and -77.8% (SOAP) to 20.0% for SOA. In Europe, the VBS_WLS produces the highest domain average OA in winter (2.3 μg $m^{-3}$), which is 106.6% and 26.2% higher than VBS_BASE and VBS_noWLS, respectively. The largest influence of vapor wall loss correction was predicted in Romania where the VBS_WLS increase the SOA by ~80% compared to VBS_noWLS due to high emissions from residential biomass burning. VBS_WLS also leads to the highest agreement with measurements for the SOA fraction in OA (fSOA) from literature.

The optimized parameterization with vapor wall loss correction in this study is expected to provide some insight to improve SOA underestimation in CTMs. Despite the overall improvement of model performance for predicting SOA, the VBS_WLS was found to increase the mean bias at specific sites compared to noWLS. To achieve a more robust parameterization and to further improve the model performance, complementary studies on S/IVOC emissions, as well as on the formation and removal mechanisms of SOA based on extensive laboratory studies and field observations with higher spatial and temporal coverage are still needed.

*Code and data availability*. The source code of the standard CAMx model is available at the RAMBOLL website (http://www.camx.com). The modified CAMx codes, as well as the source code of the MATLAB-based VBS box model are available online at https://doi.org/10.5281/zenodo.3998342

*Author Contribution*. JJ and IEH conceived the study. JJ carried out the model simulation and data analysis. GS and AB conducted the chamber measurements. NM, FC, JEP, OF and SG provided the measurement data. SA, ASHP and UB supervised the entire work development. The manuscript was prepared by JJ. All authors discussed and contributed to the final paper.

*Competing interests*. The authors declare that they have no conflict of interest.

**Acknowledgements**. We would like to thank the support of the SNF project SAOPSOAG (200021_169787). We thank the European Centre for Medium-range Weather Forecasts (ECMWF) for the meteorological data, the National Aeronautics and Space Administration (NASA) and its data-contributing agencies (NCAR, UCAR) for the TOMS and MODIS data, the global air quality model data and the TUV model. We thank the support of CAMx by RAMBOLL. Simulation of WRF and CAMx models were performed at the Swiss National Supercomputing Centre (CSCS). We thank the Aerosol, Clouds and Trace gases

https://doi.org/10.5194/gmd-2020-274
Preprint. Discussion started: 4 September 2020




Research InfraStructure (ACTRIS) and the Chemical On-Line cOmpoSition and Source Apportionment of fine aerosoL (COLOSSAL) cost action (CA16109) for support and harmonization within OA measurements and data treatments.

## References

Akherati, A., Cappa, C. D., Kleeman, M. J., Docherty, K. S., Jimenez, J. L., Griffith, S. M., Dusanter, S., Stevens, P. S., and Jathar, S. H.: Simulating secondary organic aerosol in a regional air quality model using the statistical oxidation model - Part 3: Assessing the influence of semi-volatile and intermediate-volatility organic compounds and NOx, Atmos. Chem. Phys., 19, 4561-4594, doi: 10.5194/acp-19-4561-2019, 2019.

Andreani-Aksoyoglu, S., and Keller, J.: Estimates of monoterpene and isoprene emissions from the forests in switzerland, J. Atmos. Chem, 20, 71-87, doi: 10.1007/bf01099919, 1995.

Bertrand, A., Stefenelli, G., Bruns, E. A., Pieber, S. M., Temime-Roussel, B., Slowik, J. G., Prevot, A. S. H., Wortham, H., El Haddad, I., and Marchand, N.: Primary emissions and secondary aerosol production potential from woodstoves for residential heating: Influence of the stove technology and combustion efficiency, Atmos. Environ., 169, 65-79, doi: 10.1016/j.atmosenv.2017.09.005, 2017.

Bertrand, A., Stefenelli, G., Pieber, S. M., Bruns, E. A., Temime-Roussel, B., Slowik, J. G., Wortham, H., Prévôt, A. S. H., El Haddad, I., and Marchand, N.: Influence of the vapor wall loss on the degradation rate constants in chamber experiments of levoglucosan and other biomass burning markers, Atmos. Chem. Phys. , 2018, 10915-10930, doi: 10.5194/acp-2018-40, 2018.

Bian, Q., May, A. A., Kreidenweis, S. M., and Pierce, J. R.: Investigation of particle and vapor wall-loss effects on controlled wood-smoke smog-chamber experiments, Atmos. Chem. Phys., 15, 11027-11045, doi: 10.5194/acp-15-11027-2015, 2015.

Bozzetti, C., El Haddad, I., Salameh, D., Daellenbach, K. R., Fermo, P., Gonzalez, R., Minguillon, M. C., Iinuma, Y., Poulain, L., Elser, M., Muller, E., Slowik, J. G., Jaffrezo, J. L., Baltensperger, U., Marchand, N., and Prévôt, A. S. H.: Organic aerosol source apportionment by offline-AMS over a full year in Marseille, Atmos. Chem. Phys., 17, 8247-8268, doi: 10.5194/acp-17-8247-2017, 2017.

Bruns, E. A., El Haddad, I., Slowik, J. G., Kilic, D., Klein, F., Baltensperger, U., and Prévôt, A. S. H.: Identification of significant precursor gases of secondary organic aerosols from residential wood combustion, Scientific Reports, 6, 27881, doi: 10.1038/srep27881, 2016.

Butt, E. W., Rap, A., Schmidt, A., Scott, C. E., Pringle, K. J., Reddington, C. L., Richards, N. A. D., Woodhouse, M. T., Ramirez-Villegas, J., Yang, H., Vakkari, V., Stone, E. A., Rupakheti, M., S. Praveen, P., G. van Zyl, P., P. Beukes, J., Josipovic, M., Mitchell, E. J. S., Sallu, S. M., Forster, P. M., and Spracklen, D. V.: The impact of residential combustion emissions on atmospheric aerosol, human health, and climate, Atmos. Chem. Phys., 16, 873-905, doi: 10.5194/acp-16-873-2016, 2016.

Canonaco, F., Crippa, M., Slowik, J. G., Baltensperger, U., and Prévôt, A. S. H.: SoFi, an IGOR-based interface for the efficient use of the generalized multilinear engine (ME-2) for the source apportionment: ME-2 application to aerosol mass spectrometer data, Atmos. Meas. Tech., 6, 3649-3661, doi: 10.5194/amt-6-3649-2013, 2013.

Cappa, C. D., Jathar, S. H., Kleeman, M. J., Docherty, K. S., Jimenez, J. L., Seinfeld, J. H., and Wexler, A. S.: Simulating secondary organic aerosol in a regional air quality model using the statistical oxidation model - Part 2: Assessing the influence of vapor wall losses, Atmos. Chem. Phys., 16, 3041-3059, doi: 10.5194/acp-16-3041-2016, 2016.

Ciarelli, G., Aksoyoglu, S., El Haddad, I., Bruns, E. A., Crippa, M., Poulain, L., Äijälä, M., Carbone, S., Freney, E., O'Dowd, C., Baltensperger, U., and Prévôt, A. S. H.: Modelling winter organic aerosol at the European scale with CAMx: evaluation and source apportionment with a VBS parameterization based on novel wood burning smog chamber experiments, Atmos. Chem. Phys., 17, 7653-7669, doi: 10.5194/acp-17-7653-2017, 2017a.

Ciarelli, G., El Haddad, I., Bruns, E., Aksoyoglu, S., Möhler, O., Baltensperger, U., and Prévôt, A. S. H.: Constraining a hybrid volatility basis-set model for aging of wood-burning emissions using smog chamber experiments: a box-model study based on the VBS scheme of the CAMx model (v5.40), Geosci. Model Dev., 10, 2303-2320, doi: 10.5194/gmd-10-2303-2017, 2017b.

https://doi.org/10.5194/gmd-2020-274
Preprint. Discussion started: 4 September 2020




Cohen, A. J., Brauer, M., Burnett, R., Anderson, H. R., Frostad, J., Estep, K., Balakrishnan, K., Brunekreef, B., Dandona, L., Dandona, R., Feigin, V., Freedman, G., Hubbell, B., Jobling, A., Kan, H., Knibbs, L., Liu, Y., Martin, R., Morawska, L., Pope, C. A., Shin, H., Straif, K., Shaddick, G., Thomas, M., van Dingenen, R., van Donkelaar, A., Vos, T., Murray, C. J. L., and Forouzanfar, M. H.: Estimates and 25-year trends of the global burden of disease attributable to ambient air pollution: an analysis of data from the Global Burden of Diseases Study 2015, Lancet, 389, 1907-1918, doi: 10.1016/s0140-6736(17)30505-6, 2017.

Crippa, M., Canonaco, F., Lanz, V. A., Äijälä, M., Allan, J. D., Carbone, S., Capes, G., Ceburnis, D., Dall'Osto, M., Day, D. A., DeCarlo, P. F., Ehn, M., Eriksson, A., Freney, E., Hildebrandt Ruiz, L., Hillamo, R., Jimenez, J. L., Junninen, H., Kiendler-Scharr, A., Kortelainen, A. M., Kulmala, M., Laaksonen, A., Mensah, A. A., Mohr, C., Nemitz, E., O'Dowd, C., Ovadnevaite, J., Pandis, S. N., Petäjä, T., Poulain, L., Saarikoski, S., Sellegri, K., Swietlicki, E., Tiitta, P., Worsnop, D. R., Baltensperger, U., and Prévôt, A. S. H.: Organic aerosol components derived from 25 AMS data sets across Europe using a consistent ME-2 based source apportionment approach, Atmos. Chem. Phys., 14, 6159-6176, doi: 10.5194/acp-14-6159-2014, 2014.

Dee, D. P., Uppala, S. M., Simmons, A. J., Berrisford, P., Poli, P., Kobayashi, S., Andrae, U., Balmaseda, M. A., Balsamo, G., Bauer, P., Bechtold, P., Beljaars, A. C. M., van de Berg, L., Bidlot, J., Bormann, N., Delsol, C., Dragani, R., Fuentes, M., Geer, A. J., Haimberger, L., Healy, S. B., Hersbach, H., Holm, E. V., Isaksen, L., Kallberg, P., Kohler, M., Matricardi, M., McNally, A. P., Monge-Sanz, B. M., Morcrette, J. J., Park, B. K., Peubey, C., de Rosnay, P., Tavolato, C., Thepaut, J. N., and Vitart, F.: The ERA-Interim reanalysis: configuration and performance of the data assimilation system, Q. J. Roy. Meteor. Soc., 137, 553-597, doi: 10.1002/qj.828, 2011.

Denier van der Gon, H. A. C., Bergström, R., Fountoukis, C., Johansson, C., Pandis, S. N., Simpson, D., and Visschedijk, A. J. H.: Particulate emissions from residential wood combustion in Europe – revised estimates and an evaluation, Atmos. Chem. Phys., 15, 6503-6519, doi: 10.5194/acp-15-6503-2015, 2015.

Donahue, N. M., Robinson, A. L., Stanier, C. O., and Pandis, S. N.: Coupled Partitioning, Dilution, and Chemical Aging of Semivolatile Organics, Environ. Sci. Technol., 40, 2635-2643, doi: 10.1021/es052297c, 2006.

Donahue, N. M., Robinson, A. L., and Pandis, S. N.: Atmospheric organic particulate matter: From smoke to secondary organic aerosol, Atmos. Environ., 43, 94-106, doi: 10.1016/j.atmosenv.2008.09.055, 2009.

Donahue, N. M., Epstein, S. A., Pandis, S. N., and Robinson, A. L.: A two-dimensional volatility basis set: 1. organic-aerosol mixing thermodynamics, Atmos. Chem. Phys., 11, 3303-3318, doi: 10.5194/acp-11-3303-2011, 2011.

Emery, C.: Enhanced Meteorological Modeling and Performance Evaluation for Two Texas Ozone Episodes, ENVIRON International Corporation, Novato, CA, 2001.

Fountoukis, C., Megaritis, A. G., Skyllakou, K., Charalampidis, P. E., Pilinis, C., Denier van der Gon, H. A. C., Crippa, M., Canonaco, F., Mohr, C., Prévôt, A. S. H., Allan, J. D., Poulain, L., Petäjä, T., Tiitta, P., Carbone, S., Kiendler-Scharr, A., Nemitz, E., O'Dowd, C., Swietlicki, E., and Pandis, S. N.: Organic aerosol concentration and composition over Europe: insights from comparison of regional model predictions with aerosol mass spectrometer factor analysis, Atmos. Chem. Phys., 14, 9061-9076, doi: 10.5194/acp-14-9061-2014, 2014.

Gilardoni, S., Massoli, P., Giulianelli, L., Rinaldi, M., Paglione, M., Pollini, F., Lanconelli, C., Poluzzi, V., Carbone, S., Hillamo, R., Russell, L. M., Facchini, M. C., and Fuzzi, S.: Fog scavenging of organic and inorganic aerosol in the Po Valley, Atmos. Chem. Phys., 14, 6967-6981, doi: 10.5194/acp-14-6967-2014, 2014.

Hallquist, M., Wenger, J. C., Baltensperger, U., Rudich, Y., Simpson, D., Claeys, M., Dommen, J., Donahue, N. M., George, C., Goldstein, A. H., Hamilton, J. F., Herrmann, H., Hoffmann, T., Iinuma, Y., Jang, M., Jenkin, M. E., Jimenez, J. L., Kiendler-Scharr, A., Maenhaut, W., McFiggans, G., Mentel, T. F., Monod, A., Prévôt, A. S. H., Seinfeld, J. H., Surratt, J. D., Szmigielski, R., and Wildt, J.: The formation, properties and impact of secondary organic aerosol: current and emerging issues, Atmos. Chem. Phys., 9, 5155-5236, 2009.

Hayes, P. L., Carlton, A. G., Baker, K. R., Ahmadov, R., Washenfelder, R. A., Alvarez, S., Rappenglück, B., Gilman, J. B., Kuster, W. C., de Gouw, J. A., Zotter, P., Prévôt, A. S. H., Szidat, S., Kleindienst, T. E., Offenberg, J. H., Ma, P. K., and Jimenez, J. L.: Modeling the formation and aging of secondary organic aerosols in Los Angeles during CalNex 2010, Atmos. Chem. Phys., 15, 5773-5801, doi: 10.5194/acp-15-5773-2015, 2015.

Hildebrandt Ruiz, L., and Yarwood, G.: Interactions between organic aerosol and NOy: Influence on oxidant production., University of Texas at Austin, and ENVIRON International Corporation, Novato, CA, 2013.

https://doi.org/10.5194/gmd-2020-274
Preprint. Discussion started: 4 September 2020




Hodzic, A., Jimenez, J. L., Madronich, S., Canagaratna, M. R., DeCarlo, P. F., Kleinman, L., and Fast, J.: Modeling organic aerosols in a megacity: potential contribution of semi-volatile and intermediate volatility primary organic compounds to secondary organic aerosol formation, Atmos. Chem. Phys., 10, 5491-5514, doi: 10.5194/acp-10-5491-2010, 2010.

Hodzic, A., Kasibhatla, P. S., Jo, D. S., Cappa, C. D., Jimenez, J. L., Madronich, S., and Park, R. J.: Rethinking the global secondary organic aerosol (SOA) budget: stronger production, faster removal, shorter lifetime, Atmos. Chem. Phys., 16, 7917-7941, doi: 10.5194/acp-16-7917-2016, 2016.

Horowitz, L. W., Walters, S., Mauzerall, D. L., Emmons, L. K., Rasch, P. J., Granier, C., Tie, X. X., Lamarque, J. F., Schultz, M. G., Tyndall, G. S., Orlando, J. J., and Brasseur, G. P.: A global simulation of tropospheric ozone and related tracers: Description and evaluation of MOZART, version 2, J. Geophys. Res.-Atmos, 108, D24, 4784, doi: 10.1029/2002jd002853, 2003.

Jathar, S. H., Gordon, T. D., Hennigan, C. J., Pye, H. O. T., Pouliot, G., Adams, P. J., Donahue, N. M., and Robinson, A. L.: Unspeciated organic emissions from combustion sources and their influence on the secondary organic aerosol budget in the United States, Proceedings of the National Academy of Sciences, 111, 10473-10478, doi: 10.1073/pnas.1323740111, 2014.

Jiang, J., Aksoyoglu, S., Ciarelli, G., Oikonomakis, E., El-Haddad, I., Canonaco, F., O'Dowd, C., Ovadnevaite, J., Minguillón, M. C., Baltensperger, U., and Prévôt, A. S. H.: Effects of two different biogenic emission models on modelled ozone and aerosol concentrations in Europe, Atmos. Chem. Phys., 19, 3747-3768, doi: 10.5194/acp-19-3747-2019, 2019a.

Jiang, J., Aksoyoglu, S., El-Haddad, I., Ciarelli, G., Denier van der Gon, H. A. C., Canonaco, F., Gilardoni, S., Paglione, M., Minguillón, M. C., Favez, O., Zhang, Y., Marchand, N., Hao, L., Virtanen, A., Florou, K., O'Dowd, C., Ovadnevaite, J., Baltensperger, U., and Prévôt, A. S. H.: Sources of organic aerosols in Europe: a modeling study using CAMx with modified volatility basis set scheme, Atmos. Chem. Phys., 19, 15247-15270, doi: 10.5194/acp-19-15247-2019, 2019b.

Jimenez, J. L., Canagaratna, M. R., Donahue, N. M., Prevot, A. S. H., Zhang, Q., Kroll, J. H., DeCarlo, P. F., Allan, J. D., Coe, H., Ng, N. L., Aiken, A. C., Docherty, K. S., Ulbrich, I. M., Grieshop, A. P., Robinson, A. L., Duplissy, J., Smith, J. D., Wilson, K. R., Lanz, V. A., Hueglin, C., Sun, Y. L., Tian, J., Laaksonen, A., Raatikainen, T., Rautiainen, J., Vaattovaara, P., Ehn, M., Kulmala, M., Tomlinson, J. M., Collins, D. R., Cubison, M. J., Dunlea, E. J., Huffman, J. A., Onasch, T. B., Alfarra, M. R., Williams, P. I., Bower, K., Kondo, Y., Schneider, J., Drewnick, F., Borrmann, S., Weimer, S., Demerjian, K., Salcedo, D., Cottrell, L., Griffin, R., Takami, A., Miyoshi, T., Hatakeyama, S., Shimono, A., Sun, J. Y., Zhang, Y. M., Dzepina, K., Kimmel, J. R., Sueper, D., Jayne, J. T., Herndon, S. C., Trimborn, A. M., Williams, L. R., Wood, E. C., Middlebrook, A. M., Kolb, C. E., Baltensperger, U., and Worsnop, D. R.: Evolution of Organic Aerosols in the Atmosphere, Science, 326, 1525-1529, doi: 10.1126/science.1180353, 2009.

Kanakidou, M., Seinfeld, J. H., Pandis, S. N., Barnes, I., Dentener, F. J., Facchini, M. C., Van Dingenen, R., Ervens, B., Nenes, A., Nielsen, C. J., Swietlicki, E., Putaud, J. P., Balkanski, Y., Fuzzi, S., Horth, J., Moortgat, G. K., Winterhalter, R., Myhre, C. E. L., Tsigaridis, K., Vignati, E., Stephanou, E. G., and Wilson, J.: Organic aerosol and global climate modelling: a review, Atmos. Chem. Phys., 5, 1053-1123, doi: 10.5194/acp-5-1053-2005, 2005.

Krechmer, J. E., Pagonis, D., Ziemann, P. J., and Jimenez, J. L.: Quantification of Gas-Wall Partitioning in Teflon Environmental Chambers Using Rapid Bursts of Low-Volatility Oxidized Species Generated in Situ, Environ. Sci. Technol., 50, 5757-5765, doi: 10.1021/acs.est.6b00606, 2016.

Kuenen, J. J. P., Visschedijk, A. J. H., Jozwicka, M., and Denier van der Gon, H. A. C.: TNO-MACC_II emission inventory; a multi-year (2003-2009) consistent high-resolution European emission inventory for air quality modelling, Atmos. Chem. Phys., 14, 10963-10976, doi: 10.5194/acp-14-10963-2014, 2014.

Lelieveld, J., Evans, J. S., Fnais, M., Giannadaki, D., and Pozzer, A.: The contribution of outdoor air pollution sources to premature mortality on a global scale, Nature, 525, 367, doi: 10.1038/nature15371, 2015.

Loza, C. L., Chan, A. W. H., Galloway, M. M., Keutsch, F. N., Flagan, R. C., and Seinfeld, J. H.: Characterization of Vapor Wall Loss in Laboratory Chambers, Environ. Sci. Technol., 44, 5074-5078, doi: 10.1021/es100727v, 2010.

Matsunaga, A., and Ziemann, P. J.: Gas-Wall Partitioning of Organic Compounds in a Teflon Film Chamber and Potential Effects on Reaction Product and Aerosol Yield Measurements, Aerosol Science and Technology, 44, 881-892, doi: 10.1080/02786826.2010.501044, 2010.

https://doi.org/10.5194/gmd-2020-274
Preprint. Discussion started: 4 September 2020




May, A. A., Levin, E. J. T., Hennigan, C. J., Riipinen, I., Lee, T., Collett, J. L., Jimenez, J. L., Kreidenweis, S. M., and Robinson, A. L.: Gas-particle partitioning of primary organic aerosol emissions: 3. Biomass burning, J. Geophys. Res.-Atmos, 118, 11327-11338, 2013.

Meroni, A., Pirovano, G., Gilardoni, S., Lonati, G., Colombi, C., Gianelle, V., Paglione, M., Poluzzi, V., Riva, G. M., and Toppetti, A.: Investigating the role of chemical and physical processes on organic aerosol modelling with CAMx in the Po Valley during a winter episode, Atmos. Environ., 171, 126-142, doi: 10.1016/j.atmosenv.2017.10.004, 2017.

Mitchell, M.: An Introduction to Genetic Algorithms, The MIT Press, Cambridge, Massachusetts • London, England, 1996.

NCAR: The Tropospheric Visible and Ultraviolet (TUV) Radiation Model web page, National Center for Atmospheric Research, Atmospheric Chemistry Division, Boulder, Colorado, 2011.

Nenes, A., Pandis, S. N., and Pilinis, C.: ISORROPIA: A new thermodynamic equilibrium model for multiphase multicomponent inorganic aerosols, Aquat. Geochem., 4, 123-152, doi: 10.1023/a:1009604003981, 1998.

Oderbolz, D. C., Aksoyoglu, S., Keller, J., Barmpadimos, I., Steinbrecher, R., Skjøth, C. A., Plaß-Dülmer, C., and Prévôt, A. S. H.: A comprehensive emission inventory of biogenic volatile organic compounds in Europe: improved seasonality and land-cover, Atmos. Chem. Phys., 13, 1689-1712, doi: 10.5194/acp-13-1689-2013, 2013.

Paglione, M., Gilardoni, S., Rinaldi, M., Decesari, S., Zanca, N., Sandrini, S., Giulianelli, L., Bacco, D., Ferrari, S., Poluzzi, V., Scotto, F., Trentini, A., Poulain, L., Herrmann, H., Wiedensohler, A., Canonaco, F., Prévôt, A. S. H., Massoli, P., Carbone, C., Facchini, M. C., and Fuzzi, S.: The impact of biomass burning and aqueous-phase processing on air quality: a multi-year source apportionment study in the Po Valley, Italy, Atmos. Chem. Phys., 20, 1233-1254, doi: 10.5194/acp-20-1233-2020, 2020.

Pankow, J. F.: An absorption model of gas/particle partitioning of organic compounds in the atmosphere, Atmos. Environ., 28, 185-188, doi: 10.1016/1352-2310(94)90093-0, 1994.

Qi, L., Chen, M., Stefenelli, G., Pospisilova, V., Tong, Y., Bertrand, A., Hueglin, C., Ge, X., Baltensperger, U., Prévôt, A. S. H., and Slowik, J. G.: Organic aerosol source apportionment in Zurich using an extractive electrospray ionization time-of-flight mass spectrometer (EESI-TOF-MS) – Part 2: Biomass burning influences in winter, Atmos. Chem. Phys., 19, 8037-8062, doi: 10.5194/acp-19-8037-2019, 2019.

Ramboll: User's guide: the Comprehensive Air Quality Model with extensions (CAMx) version 6.5, California, 2018.

Robinson, A. L., Donahue, N. M., Shrivastava, M. K., Weitkamp, E. A., Sage, A. M., Grieshop, A. P., Lane, T. E., Pierce, J. R., and Pandis, S. N.: Rethinking Organic Aerosols: Semivolatile Emissions and Photochemical Aging, Science, 315, 1259-1262, doi: 10.1126/science.1133061, 2007.

Skamarock, W. C., Klemp, J. B., Dudhia, J., Gill, D. O., Barker, D. M., Duda, M. G., Huang, X.-Y., Wang, W., and Powers, J. G.: A Description of the Advanced Research WRF Version 3, Mesoscale and Microscale Meteorology Division, National Center for Atmospheric Research, Boulder, Colorado, USA, 2008.

Stefenelli, G., Jiang, J., Bertrand, A., Bruns, E. A., Pieber, S. M., Baltensperger, U., Marchand, N., Aksoyoglu, S., Prévôt, A. S. H., Slowik, J. G., and El Haddad, I.: Secondary organic aerosol formation from smoldering and flaming combustion of biomass: a box model parametrization based on volatility basis set, Atmos. Chem. Phys., 19, 11461-11484, doi: 10.5194/acp-19-11461-2019, 2019.

Tsimpidi, A. P., Karydis, V. A., Zavala, M., Lei, W., Molina, L., Ulbrich, I. M., Jimenez, J. L., and Pandis, S. N.: Evaluation of the volatility basis-set approach for the simulation of organic aerosol formation in the Mexico City metropolitan area, Atmos. Chem. Phys., 10, 525-546, 2010.

Woody, M. C., West, J. J., Jathar, S. H., Robinson, A. L., and Arunachalam, S.: Estimates of non-traditional secondary organic aerosols from aircraft SVOC and IVOC emissions using CMAQ, Atmos. Chem. Phys., 15, 6929-6942, doi: 10.5194/acp-15-6929-2015, 2015.

Zhang, X., Cappa, C. D., Jathar, S. H., McVay, R. C., Ensberg, J. J., Kleeman, M. J., and Seinfeld, J. H.: Influence of vapor wall loss in laboratory chambers on yields of secondary organic aerosol, Proceedings of the National Academy of Sciences, 111, 5802-5807, doi: 10.1073/pnas.1404727111, 2014.

Zhang, Y., Favez, O., Petit, J. E., Canonaco, F., Truong, F., Bonnaire, N., Crenn, V., Amodeo, T., Prévôt, A. S. H., Sciare, J., Gros, V., and Albinet, A.: Six-year source apportionment of submicron organic aerosols from near-continuous highly time-resolved measurements at SIRTA (Paris area, France), Atmos. Chem. Phys., 19, 14755-14776, doi: 10.5194/acp-19-14755-2019, 2019.

https://doi.org/10.5194/gmd-2020-274
Preprint. Discussion started: 4 September 2020


Geoscientific Model Development Discussions

**Table 1:** Statistical results for model performance on simulating OA, SOA and POA. The number of daily average observations from five ACSM/AMS stations is 232.

| Species | OA scheme | MB (μg $m^{-3}$) | ME (μg $m^{-3}$) | RMSE (μg $m^{-3}$) | MFB (%) | MFE (%) |
|---|---|---|---|---|---|---|
| OA | SOAP | -4.1 | 4.9 | 7.2 | -44.3 | 65.3 |
| | VBS_BASE | -4.9 | 5.6 | 7.9 | -72.9 | 83.3 |
| | VBS_3POA | -1.6 | 4.3 | 6.5 | -12.4 | 51.7 |
| | VBS_noWLS | -1.9 | 4.3 | 6.5 | -17.4 | 52.7 |
| | VBS_WLS | -0.4 | 4.6 | 6.9 | -1.6 | 52.2 |
| SOA | SOAP | -2.3 | 3.1 | 4.3 | -77.8 | 98.3 |
| | VBS_BASE | -1.6 | 2.8 | 4.1 | -63.0 | 90.6 |
| | VBS_3POA | -1.2 | 2.8 | 4.1 | -51.1 | 84.3 |
| | VBS_noWLS | -1.3 | 2.8 | 4.0 | -52.5 | 84.9 |
| | VBS_WLS | 0.2 | 3.2 | 4.6 | -20.0 | 76.4 |
| POA | SOAP | -0.7 | 1.9 | 3.1 | 4.4 | 56.7 |
| | VBS_BASE | -2.3 | 2.5 | 4.0 | -64.1 | 81.5 |
| | VBS_3POA | 0.8 | 2.4 | 3.4 | 36.3 | 64.2 |
| | VBS_noWLS | 0.4 | 2.2 | 3.2 | 30.1 | 61.9 |
| | VBS_WLS | 0.6 | 2.3 | 3.3 | 32.4 | 62.5 |

545

https://doi.org/10.5194/gmd-2020-274
Preprint. Discussion started: 4 September 2020


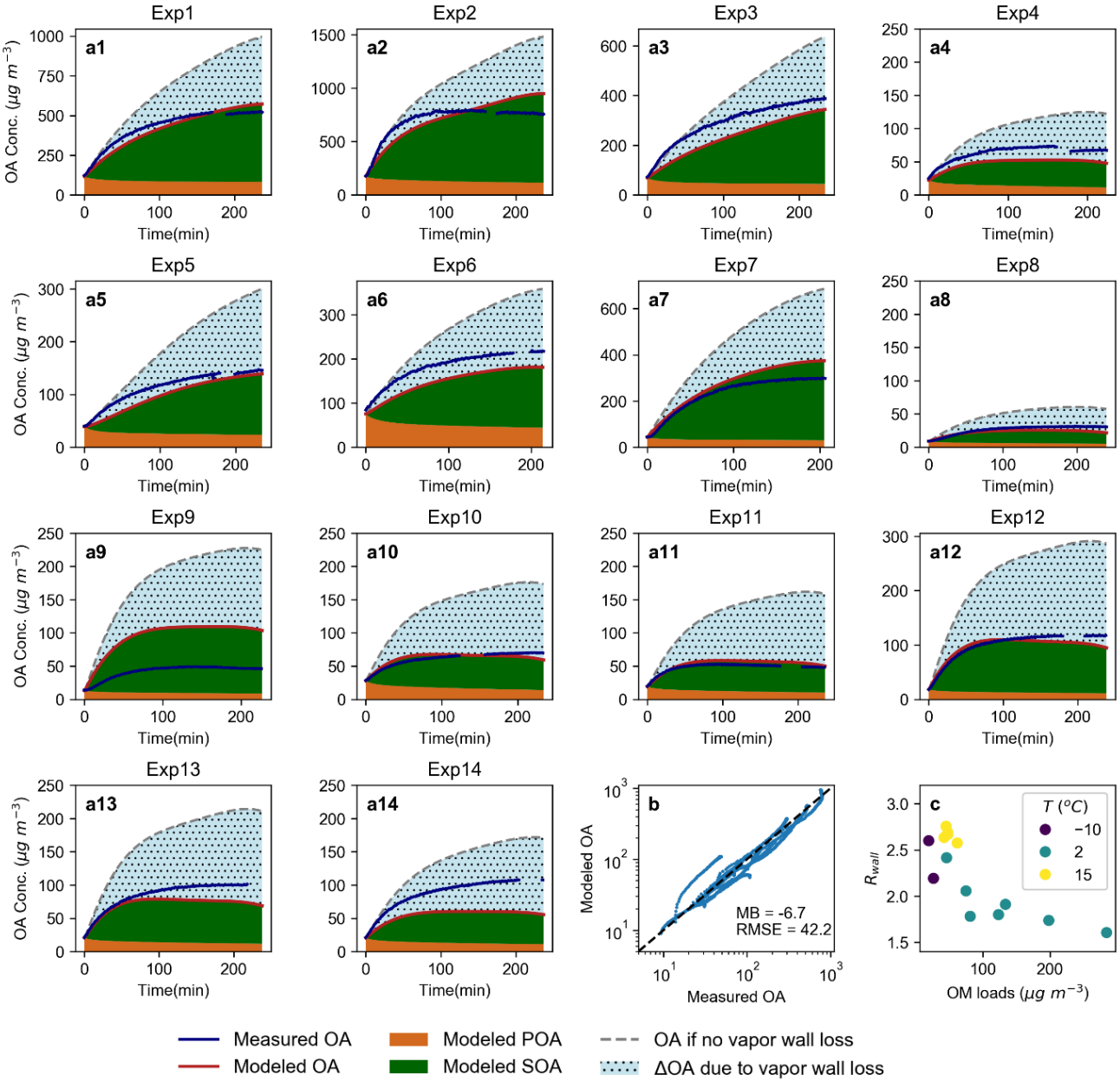


**Figure 1:** Comparison between measured and modeled OA with optimized parameterization under $k_w$ = 0.0033 $s^{-1}$, $C_{wall}$ = 5 mg $m^{-3}$ (a, b) and relation between the endpoint wall loss factor $R_{wall}$ of each experiment and initial OM loads under different temperature (c). The gray dashed lines in (a) represent modeled OA with the same parameterization but set $k_w$=0.

550

https://doi.org/10.5194/gmd-2020-274
Preprint. Discussion started: 4 September 2020


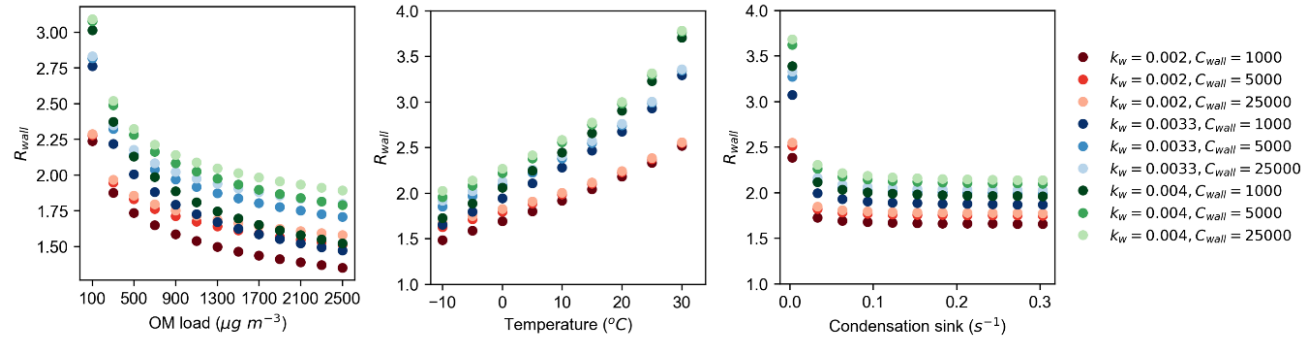


**Figure 2:** Dependence of wall loss factor $R_{wall}$ ($C_{OA,\ kw=0}$ /$C_{OA,\ optimal\ kw}$) on initial organic mass load, temperature and condensation sink.

555

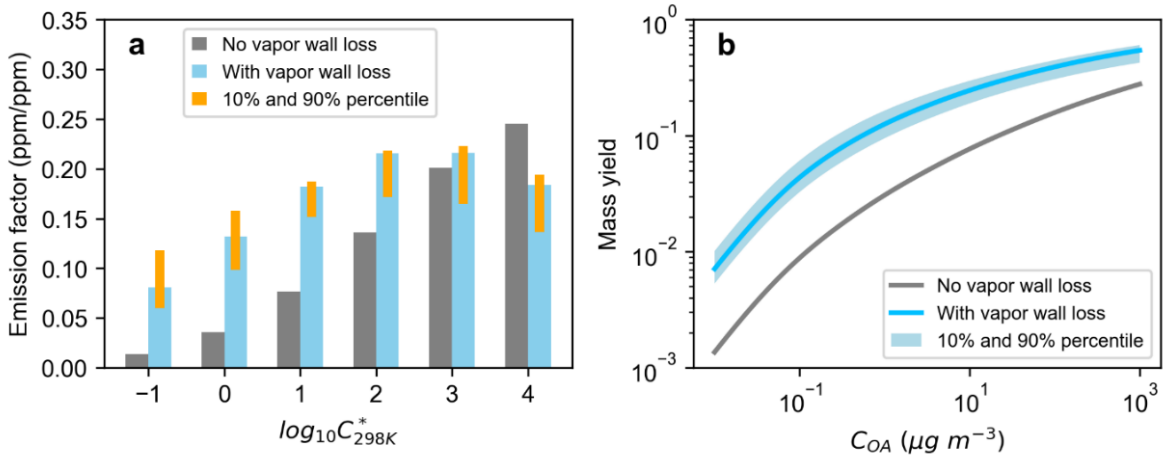


**Figure 3:** Optimized emission factors (a) and mass yield of SOA from biomass burning at 298 K (b) with and without vapor wall loss correction. The blue bars (a) and line (b) with vapor wall loss refer to median chamber conditions with $k_w$ = 0.0033 $s^{-1}$, $C_{wall}$ = 5 mg $m^{-3}$.

560

https://doi.org/10.5194/gmd-2020-274
Preprint. Discussion started: 4 September 2020


Geoscientific Model Development Discussions

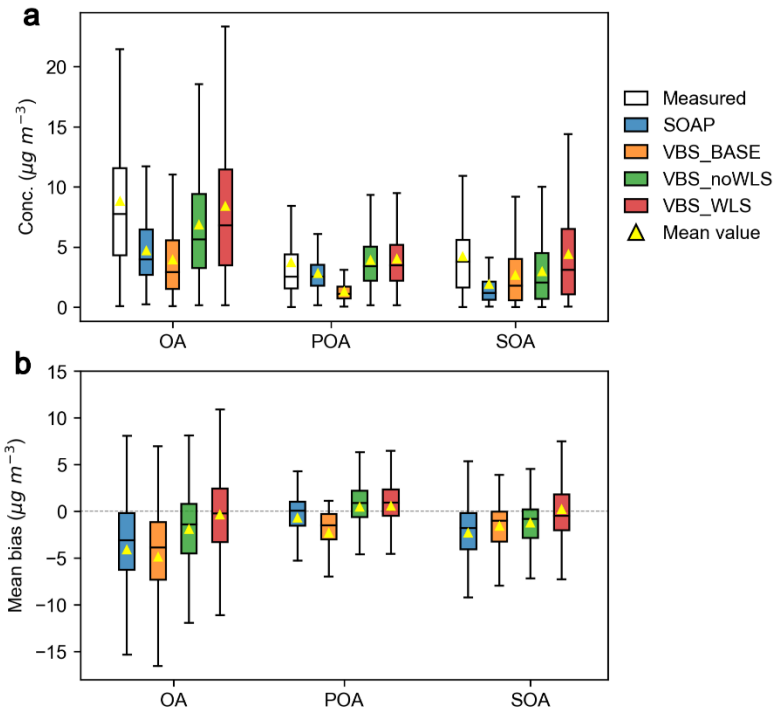


**Figure 4:** Concentrations of measured and modeled OA, POA and SOA at five ACSM/AMS stations in winter (a) and mean bias for different OA schemes (b). The lines inside boxes represent median values, and the yellow triangles represent mean values.

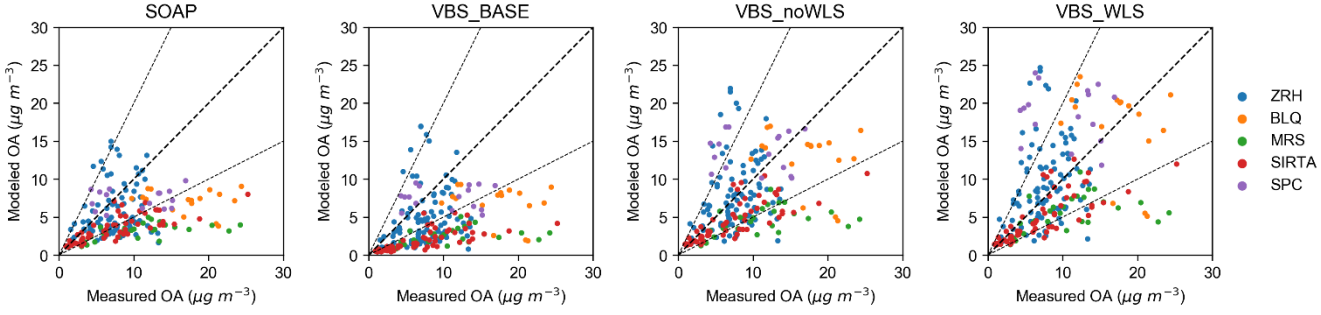


**Figure 5:** Measured and modeled daily average OA using different OA schemes in winter. ZRH: Zurich, BLQ: Bologna, MRS: Marseille, SIRTA: Paris SIRTA, SPC: San Pietro Capofiume.

https://doi.org/10.5194/gmd-2020-274
Preprint. Discussion started: 4 September 2020


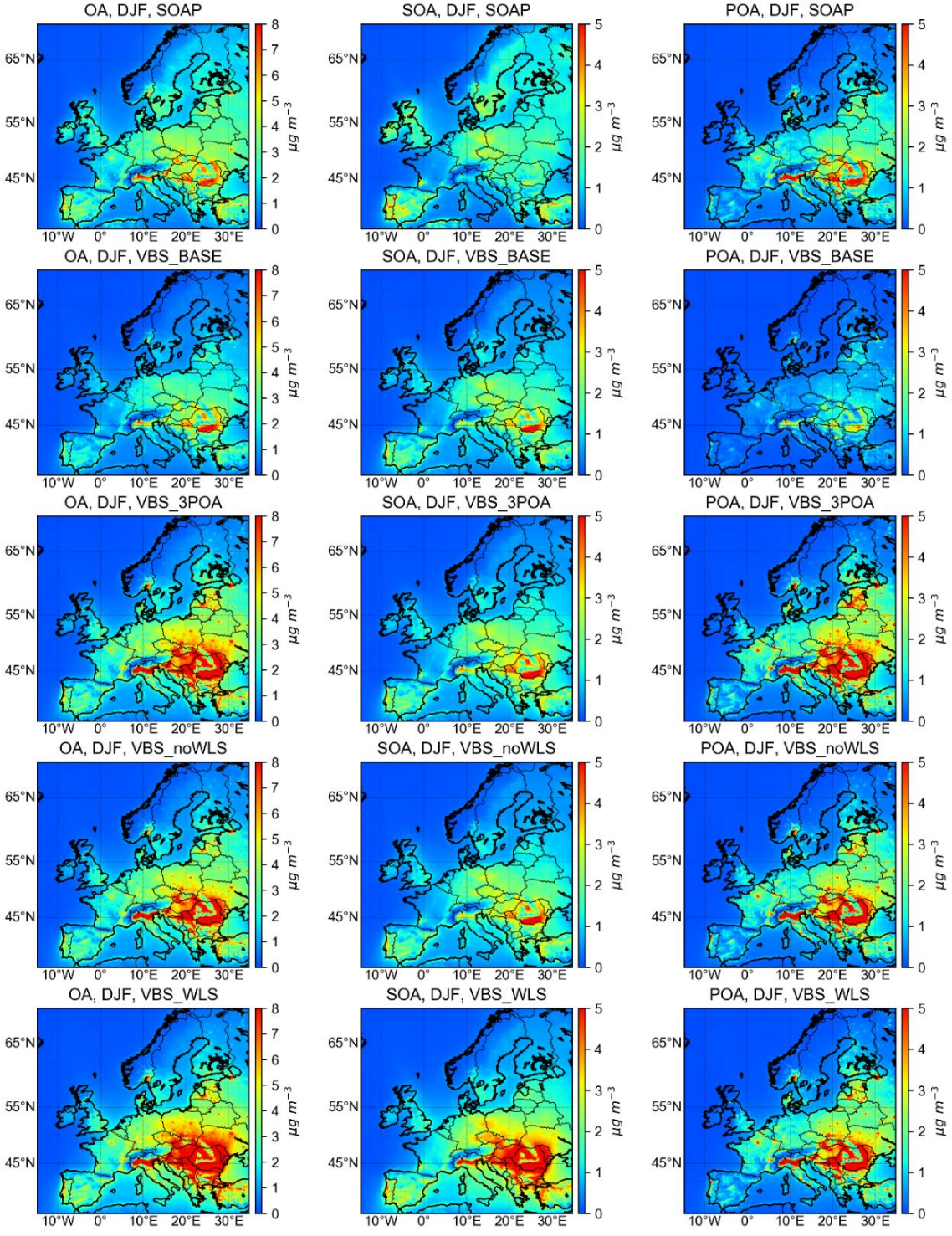


**Figure 6:** Modeled OA, SOA and POA in winter (DJF, December–January–February) by different OA schemes.

https://doi.org/10.5194/gmd-2020-274
Preprint. Discussion started: 4 September 2020


Geoscientific Model Development Discussions

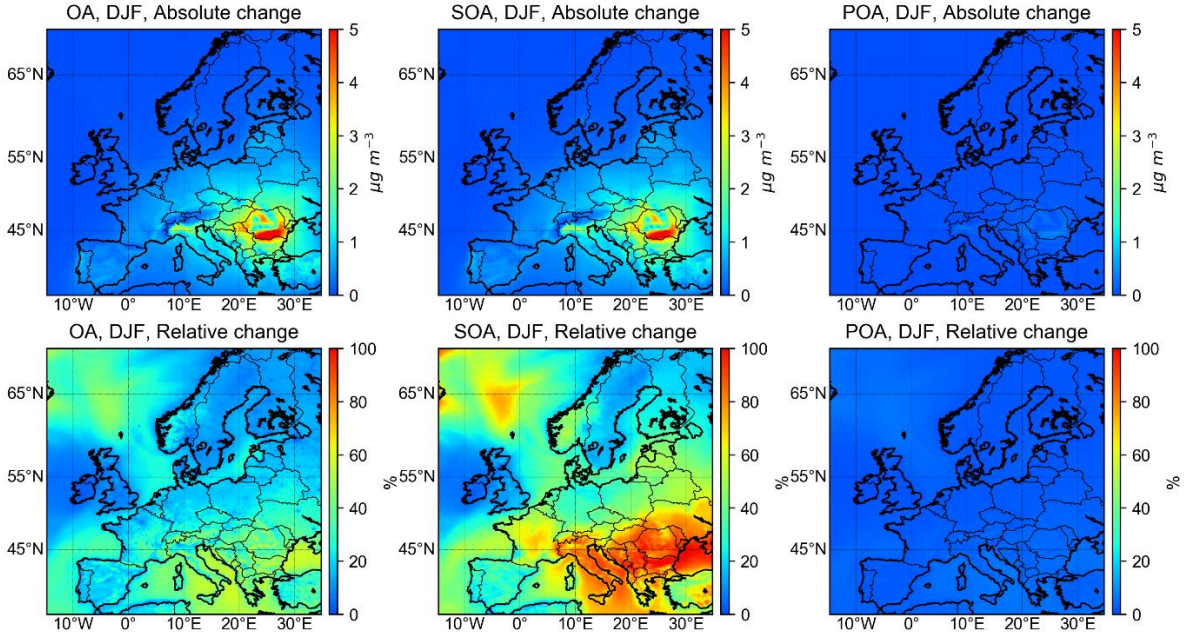


575 **Figure 7:** Differences in modeled OA, SOA and POA in winter (DJF, December–January–February) by VBS schemes with (VBS_WLS) and without (VBS_noWLS) vapor wall corrections.

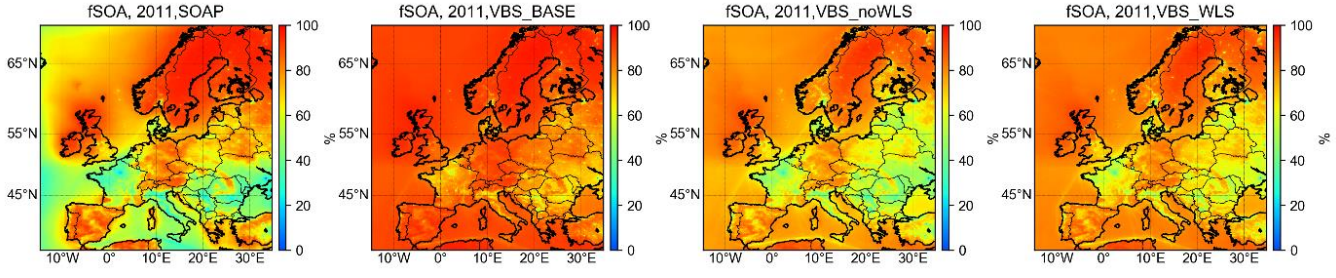


580 **Figure 8:** Modeled fractions of SOA to total OA (fSOA) using different OA schemes. Modeled results of VBS_3POA are very similar to VBS_noWLS, and therefore are not shown here.

https://doi.org/10.5194/gmd-2020-274
Preprint. Discussion started: 4 September 2020


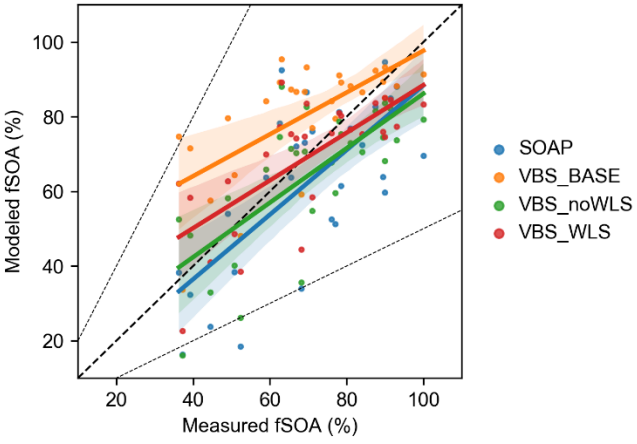


**Figure 9:** Comparison between modeled and measured fSOA from literature (see data and sources in Table S1). The shadows are confidence intervals of the regression lines.